Appendix A
Positive and Negative Frequency

In this appendix, we will discuss further arguments in favour of the consideration of the sign of frequency of a mode of a field. The discussion will be based on the study of sinusoidal functions.

Sinusoidal functions

A sinusoid is a function of the form

$$x(t) = A\sin(\omega t + \phi), \tag{A.1}$$

where t is an independent (real) variable, and the fixed parameters A (the amplitude), ω (the radian frequency), and ϕ (the initial phase) are all real constants. The argument of the sine function, $\omega t + \phi$ is referred to as the instantaneous phase. Since the sine function is periodic with period 2π, the range of the initial phase is usually restricted to any values between 0 and 2π. The radian frequency ω is the time derivative of the instantaneous phase—$\omega = \frac{d}{dt}(\omega t + \phi)$.

A sinusoid's frequency content may be graphed in the frequency domain by representing its spectral magnitude by (unit-amplitude, and ϕ=0 case)

$$\sin(\omega_x t) = \frac{1}{2i}e^{i\omega_x t} - \frac{1}{2i}e^{-i\omega_x t}. \tag{A.2}$$

That is, the spectrum of a unit-amplitude sinusoid of radian frequency ω_x (and phase $\pi/2$) consists of two components with amplitude $1/2$, one at frequency $\omega_x/2\pi$ and the other at frequency $-\omega_x/2\pi$.

Complex sinusoids

We define the complex sinusoid from Euler's Identity

$$e^{i(\omega t+\phi)} = \cos(\omega t + \phi) + i\sin(\omega t + \phi), \tag{A.3}$$

by multiplying it with an amplitude $A > 0$

M. J. Jacquet, *Negative Frequency at the Horizon*, Springer Theses,
https://doi.org/10.1007/978-3-319-91071-0

$$Ae^{i(\omega t+\phi)} = A\cos(\omega t+\phi) + iA\sin(\omega t+\phi). \tag{A.4}$$

From this equation, we see that a complex sinusoid consists of a real part and an imaginary part—its in-phase and phase-quadrature components, respectively. A complex sinusoid has a constant modulus—a constant complex magnitude.

Given its constant modulus, a complex sinusoid must lie on a circle in the complex plane: a positive-frequency sinusoid ($e^{i\omega t}$, $\omega > 0$) traces out counter-clockwise circular motion along the unit circle as t increases, while a negative-frequency sinusoid ($e^{-i\omega t}$, $\omega > 0$) traces out a clockwise circular motion.[1]

Positive-and negative-frequencies components of a real field

By Euler's Identity, all real sinusoids consist of a sum of opposite circular motion: this is best seen by writing out

$$\sin(\omega t+\phi) = \frac{e^{i(\omega t+\phi)} - e^{-i(\omega t+\phi)}}{2i}. \tag{A.5}$$

It is obvious that every real sinusoid consists of an equal contribution of positive- and negative-frequency components.[2] Spectrum analysis [1] tells us that every real signal contains equal amounts of positive and negative frequencies. If we denote the spectrum of the real signal $x(t)$ by $X(\omega)$, we have

$$|X(-\omega)| = |X(\omega)|. \tag{A.6}$$

So why do we usually not consider the negative frequency component of real signals? Well, it is because complex sinusoids have a constant modulus: amplitude envelope detectors (typically, power meters) "compute" the square root of the sum of the squares of the real and imaginary part of the signal to obtain the instantaneous peak amplitude. In other words, we usually convert real sinusoids into complex ones, by removing the negative-frequency component, before processing them.

[1] Note that both positive- and negative-frequency sinusoids are necessarily complex.

[2] A real sinusoid is the sum of a positive-frequency and a negative-frequency complex sinusoid.

Appendix B
Modelling of a Change in the Dielectric Constant

In this section of the appendix, we will comment further on the modelling of the dielectric constant in the Sellmeier model, and the modification of this dielectric constant when the refractive index is increased (e.g. by the Kerr effect in the fibre optical experiment of Chap. 5 of this dissertation).

Sellmeier coefficients in the Hopfield model

In Sect. 3.2.3, I explained how the Sellmeier coefficients (the resonance frequency $\omega_i = \frac{2\pi c}{\lambda_i}$ and elastic constant κ_i) of the medium (a set of polarisation fields modelled by harmonic oscillators) were modified by the frequency-dependent change in the refractive index under the step of height δn (as illustrated in Fig. 3.4) by Eq. (3.71). I argued that, in the light of the present lack of theoretical description of the collection of quantum processes from which the dielectric constant of a material arises, the Hopfield model of the dielectric [2] was only an approximation of physical reality. In a scheme based on this approximation, the modulation by (3.71) of the Sellmeier coefficients is a usual description of the change in the dielectric constant within a self-consistent theory.

The question then arises of which of the two coefficients, the resonant frequency or the elastic constant, should be modified to best account for the change in the dielectric constant. I argued that we do not, at present, have at our disposal a good theoretical argument that would discriminate between the two effects—or indeed a combination of both, as proposed in [3, 4] and used in this Thesis and [5].

At the onset of their study, one thus has to make a choice as to which modification to make: either κ_i or ω_i, or both κ_i and ω_i, are modified by the change in the refractive index (of amplitude δn)—note that, in any case, this change has to be frequency dependent. From this choice stem the matching conditions. As I demonstrated in Sect. 3.2.4, if κ_i is to be modified by δn (independently of the modification of ω_i), then there is a discontinuity in the elastic constant at the interface. On the other hand, even if ω_i is modified by δn (independently of the modification of κ_i), this does not create a discontinuity at the interface (the resonant frequency is continuous at the interface for any amplitude of δn). So the choice mentioned above influences the matching conditions, and thus it influences the scattering matrix (because the

M. J. Jacquet, *Negative Frequency at the Horizon*, Springer Theses,
https://doi.org/10.1007/978-3-319-91071-0

elements of the matrix stem from the matching conditions and the amplitude of the modes at the interface).

Dispersion relation

I think that this Thesis demonstrated how the structure and shape of the dispersion relation influence the spectra of emission at the refractive index front (RIF). With this in mind, I would argue that looking at the dispersion relation, which can be readily calculated for any of the three cases we are interested in, may shed some light on the impact of the modification of the Sellmeier coefficients on the spectra of spontaneous emission. For simplicity, we will here focus on the optical branch, and the modes of optical frequency (of positive and negative norm).

Figure B.1 displays the positive-norm optical branch of the dispersion relation in the laboratory frame, and the positive- and negative-norm optical branch in the moving frame (the frame co-moving with the RIF at velocity $u = 0.66c$). The branches are shown in the low- and high-refractive-index region, for $\delta n = 0.048$ at the step. We see that, as only the resonant frequency ω_i is changed by the increase in the refractive index, the distance in the laboratory frame (Fig. B.1a) between the optical branch in the low- and high-refractive-index regions is largest around $k = 0$ and at large $|k|$. In the moving frame (Fig. B.1d), the positive- and negative-norm branches in the high-refractive-index region are very close to their low-refractive-index region counterparts. Thus we expect the moving frame frequency intervals over which the RIF acts as a black-hole and a white-hole to be very narrow. The situation is almost exactly opposite in the case in which only the elastic constant κ_i is changed by the increase in the refractive index (Fig. B.1b), the branch in the high refractive index region overlaps with that in the low refractive index region around $k = 0$ and at large $|k|$, and is furthest away in the medium $|k|$ regime. In the moving frame (Fig. B.1e), the high-refractive-index region branches (of positive- and negative-norm) are far from overlapping with the low-refractive-index region one. Thus we expect the moving frame frequency intervals over which the RIF acts as a black-hole and a white-hole to be relatively large—comparably to the case in which both the Sellmeier coefficients are modified, as discussed in Chaps. 3 and 4 and plotted in Fig. B.1c and f for comparison.

Note that the overall curvature of the dispersion relation does not seem to be affected by the independent change in the Sellmeier coefficients. Thus it is reasonable to assume that the shape of the spontaneous emission spectra will not drastically change either. That is, they should exhibit the same horizon-like features (such as the "shark fin") as those presented in Chap. 4.

Spectra of emission

The algorithm presented in Chap. 4 is based on the matching conditions found in Sect. 3.2.4: it allows for calculating the scattering matrix if the elasticity κ_i is discontinuous, and if the resonant frequency ω_i is continuous, at the interface *only*. This means that, unfortunately, the case of continuous (unchanged) κ_i cannot be investigated without modifying the algorithm, after having found out about the new analytical expression for the matching conditions and relations between Global Modes

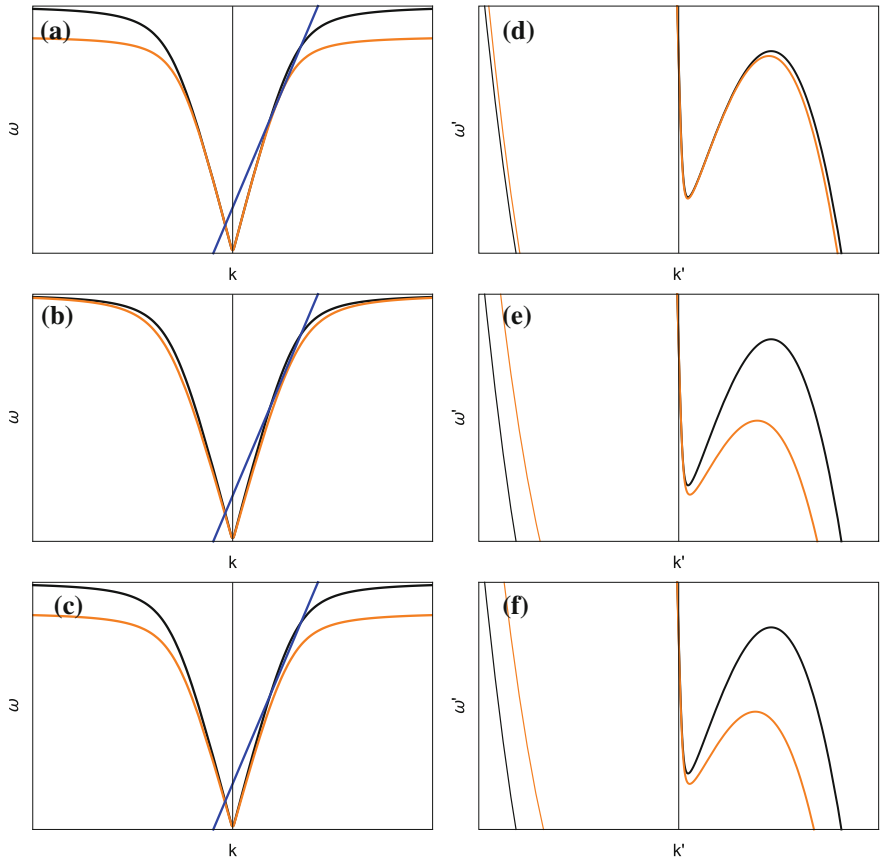

Fig. B.1 Change of elasticity and/or resonance frequency by refractive index increase. Left column: positive-norm optical branch in the laboratory frame; right column: positive- and negative-norm optical branch in the moving frame. The branches are shown in the low refractive index region (black) and high refractive index region (orange), with $\delta n = 0.048$ in bulk fused silica. In (**a**) and (**d**), only the resonant frequencies ω_1 and ω_2 are changed; in (**b**) and (**e**), only the elastic constants κ_1 and κ_2 are changed; in (**c**) and (**e**), both the resonant frequencies ω_1 and ω_2 and elastic constants κ_1 and κ_2 are changed (as in Chaps. 3 and 4). A contour line of constant moving frame frequency ω' is shown on the laboratory frame dispersion plots (a, b and c) to aid the visualisation of the change in the Sellmeier coefficients

(GM) in the inhomogeneous medium. Thus, spectra in the case of unchanged κ_i and changed ω_i cannot be computed presently. On the other hand, it is possible to compute spectra in the case of changed κ_i and unchanged ω_i can be—and the case in which both are affected by the increase in the refractive index was the subject of Sect. 4.3.

I here present new numerical results that allow for comparing the impact of changing both κ_i and ω_i, or changing solely κ_i. The moving-frame photonic flux in the negative-norm optical mode *noL* and the uniquely escaping mode *moR* (that has a

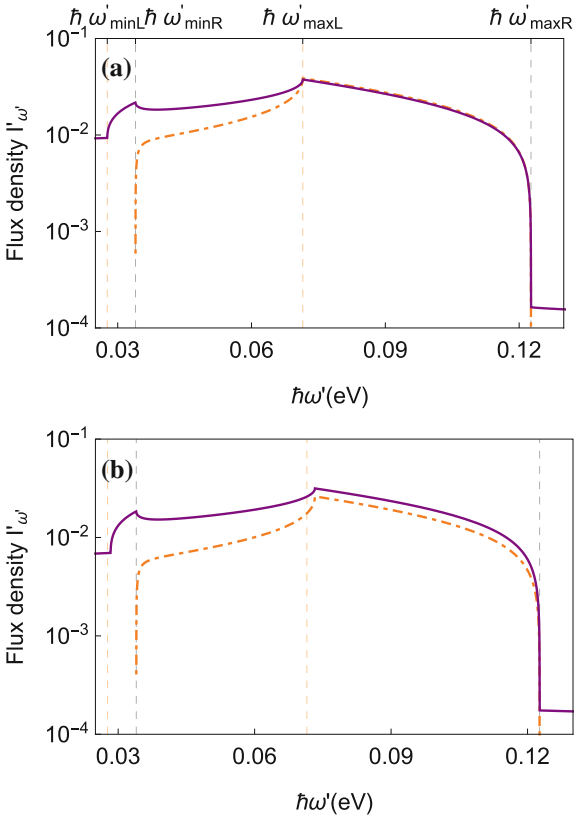

Fig. B.2 Emission spectra of optical modes of positive- and negative-norm in the moving frame in bulk fused silica. The flux density in mode *noL* (purple curve) and *moR* (orange-dashed curve) is shown for a step height $\delta n = 0.048$. In **a** both the Sellmeier coefficients are modified (as in Fig. 4.6d) and in **b** only the elastic constants κ_1 and κ_2 are modified. The vertical dotted lines in both (**a**) and (**b**) indicate the limits of the subluminal intervals when both Sellmeier coefficients are modified by a $\delta n = 0.048$ (Fig. 4.6d)

positive norm) are shown in Fig. B.2 when both Sellmeier coefficients are modified in (a), and when only κ_i is modified in (b). As anticipated in the above paragraph, the overall shape of the spectra is not significantly affected by the fact that the resonant frequency is not changed in Fig. B.2b). Horizontal lines indicating the limits of the subluminal intervals (see Sect. 3.2.3) when both Sellmeier coefficients are modified are shown for reference. When only the elastic constant is modified, the characteristic features of the spectra ("shark fin") are slightly shifted to higher frequencies, and it seems that the emission is overall weaker. Moreover, the emission in *noL* is stronger than in *moR* over the black-hole interval (between $\hbar\omega'_{maxL}$ and $\hbar\omega'_{maxR}$), which is a departure from the equality of the fluxes observed when both Sellmeier coefficients are modified to model the frequency-dependent change in the refractive index.

From these spectra, it is sound to assume that the spectrum of emission when only the resonant frequency of the medium would be modified would feature the same shark fin features (and possibly lower flux amplitudes), although over narrower intervals. The spectrum would then be appreciably different from those presented on Fig. B.2. Such numerical calculations should definitely be carried to check those predictions.

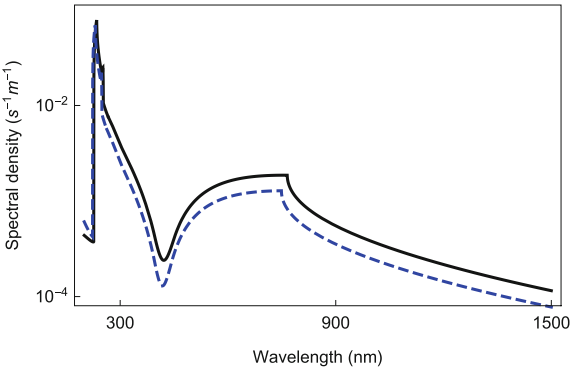

Fig. B.3 Laboratory Spectral Density with modified Sellmeier coefficients. Spectra are calculated for a step of height $\delta n = 0.048$ in bulk fused silica. Dashed-blue: spectrum when κ_1 and κ_2 only are modified; black: spectrum when both Sellmeier coefficients are modified

I also calculated the density of spectral emission in the laboratory frame in the case in which only κ_i is modified to account for the frequency-dependent change in the refractive index under the step of height $\delta n = 0.048$. The LSD is shwon in blue in Fig. B.3: we see that it is mostly similar to the reference spectrum obtained in Sect. 4.3.2, shown here in black. As for the moving frame spectra, the emission is mostly lower when only the elastic constant is modified, and the horizon features are blue-shifted with respect to the reference spectrum.

From these spectra, it is unclear that an optical experiment in glass would allow for clearly distinguishing the best theoretical model (modification of either or both of the Sellmeier coefficients). As I already said in the body of the dissertation, the present theory of the dielectric constant by means of the Hopfield model, and of its modification by an increase in the refractive index by modification of the Sellmeier coefficients has not to be taken too literally: modifying either or both of the elastic constant and resonance frequency is merely a means to account for the frequency dependent change in the refractive index. Unfortunately, the present theory does not account for the collection of quantum processes that would accurately describe the dielectric constant. Further study could be dedicated to extensively studying this puzzle, but for the sake of the present Thesis, modifying both κ_i and ω_i is good enough.

Appendix C
Scattering at a Smooth Profile in a Nondispersive Medium

In this appendix, I demonstrate how to calculate the wave equation for the one dimensional motion of a particle in the field of potential $U(x)$,

$$U(x) = \frac{U_0}{\cosh^2 \alpha x}. \tag{C.7}$$

I then shown how to calculate the coefficients of scattering (reflection and transmission) at such a smooth profile.

Exact solution

The one dimensional motion of a quantum particle in the field of potential $U(x)$ is described by the Schrödinger equation

$$\frac{d^2\Psi}{dx^2} + \frac{2m}{\hbar^2}\left(E - U(x)\right)\Psi = 0. \tag{C.8}$$

In the present case, this reads

$$\frac{d^2\Psi}{dx^2} + 2m\left(E - \frac{U_0}{\cosh^2 \alpha x}\right)\Psi = 0. \tag{C.9}$$

If we take

$$\xi = \tanh(x), \tag{C.10}$$

where we have implicitly rescaled the problem so that $x \to \alpha x$, then

$$\xi = \frac{\sinh(x)}{\cosh(x)} = \frac{\sqrt{\cosh^2(x) - 1}}{\cosh(x)} \tag{C.11}$$

and

$$\frac{d\xi}{dx} = \xi' = \tanh'(x) = 1 - \xi^2 = \cosh^{-2}(x). \tag{C.12}$$

M. J. Jacquet, *Negative Frequency at the Horizon*, Springer Theses,
https://doi.org/10.1007/978-3-319-91071-0

Thus we get

$$\left(\frac{d}{dx}\right)^2\Psi=\frac{d}{dx}\frac{d}{d\xi}\Psi\frac{d\xi}{dx}=\frac{d}{dx}\left[\left(1-\xi^2\right)\frac{d\Psi}{d\xi}\right]=\left(1-\xi^2\right)\left[\left(1-\xi^2\right)\frac{d\Psi}{d\xi}\right] \quad \text{(C.13)}$$

and Eq. (C.9) can be written as a function of ξ:

$$\begin{aligned}&\alpha^2\left(1-\xi^2\right)\frac{d}{d\xi}\left[\left(1-\xi^2\right)\frac{d\Psi}{d\xi}\right]+\frac{2m}{\hbar^2}\left(E-U_0\left(1-\xi^2\right)\right)\Psi=0\\&\rightarrow\frac{d}{d\xi}\left[\left(1-\xi^2\right)\frac{d\Psi}{d\xi}\right]+\left(\frac{2mE}{\hbar^2\alpha^2}\frac{1}{1-\xi^2}-\frac{2m}{\hbar^2\alpha^2}U_0\right)\Psi=0.\end{aligned} \quad \text{(C.14)}$$

Using the replacements $k=\frac{\sqrt{2mE}}{\hbar}$, and $s=\frac{1}{2}\left(\sqrt{1-\frac{8mU_0}{\alpha^2\hbar^2}}-1\right)$, and noting that $s(s+1)=-\frac{2mU_0}{\alpha^2\hbar^2}$, the Schrödinger equation (C.14) can be expressed as

$$\frac{d}{d\xi}\left[\left(1-\xi^2\right)\frac{d\Psi}{d\xi}\right]+\left(\frac{k^2}{\alpha^2}\frac{1}{1-\xi^2}+s(s+1)\right)\Psi=0. \quad \text{(C.15)}$$

This equation can also be written under a hyper-geometric form by making the substitution $\Psi=\left(1-\xi^2\right)^{-\frac{ik}{2\alpha}}\omega(\xi)$. Equation (C.15) becomes

$$\frac{d}{d\xi}\left[\left(1-\xi^2\right)\frac{d}{d\xi}\left[\left(1-\xi^2\right)^{-\frac{ik}{2\alpha}}\omega(\xi)\right]\right]+\left(\frac{k^2}{\alpha^2}\frac{1}{1-\xi^2}+s(s+1)\right)\left(\left(1-\xi^2\right)^{-\frac{ik}{2\alpha}}\omega(\xi)\right)=0. \quad \text{(C.16)}$$

The computation of the first term of the above equation yields

$$\begin{aligned}1^{st}\text{ term}&=\frac{d}{d\xi}\left[\left(1-\xi^2\right)\left(\xi\frac{ik}{\alpha}\left(1-\xi^2\right)^{-\frac{ik}{2\alpha}-1}\omega(\xi)+\left(1-\xi^2\right)^{-\frac{ik}{2\alpha}}\omega'(\xi)\right)\right]\\&=\frac{d}{d\xi}\left[\xi\frac{ik}{\alpha}\left(1-\xi^2\right)^{-\frac{ik}{2\alpha}}\omega(\xi)+\left(1-\xi^2\right)^{1-\frac{ik}{2\alpha}}\omega'(\xi)\right]\\&=\frac{ik}{\alpha}\left(1-\xi^2\right)^{-\frac{ik}{2\alpha}}\omega(\xi)-\xi^2\frac{k^2}{\alpha^2}\left(1-\xi^2\right)^{-\frac{ik}{2\alpha}-1}\omega(\xi)+\\&+\xi\frac{ik}{\alpha}\left(1-\xi^2\right)^{1-\frac{ik}{2\alpha}}\omega'(\xi)+\\&+(-2\xi)\left(1-\frac{ik}{\alpha}\right)\left(1-\xi^2\right)^{-\frac{ik}{2\alpha}}\omega'(\xi)+\left(1-\xi^2\right)^{1-\frac{ik}{2\alpha}}\omega"(\xi).\end{aligned} \quad \text{(C.17)}$$

Substituting back into Eq. (C.16) and dividing by $\left(1-\xi^2\right)^{-\frac{ik}{2\alpha}}$ yields

$$-\omega\left(-\frac{ik}{\alpha}-s^2-s+\frac{k^2}{\alpha^2}\right)-2\xi\left(1-\frac{ik}{\alpha}\right)\omega'+\left(1-\xi^2\right)\omega"=0. \tag{C.18}$$

Finally, momentarily changing the variable to $u=\frac{1}{2}(1-\xi)$, and expressing ω as a function of u - $\omega'=-2\omega'(u)$ and $\omega"=4\omega"(u)$ - leads to the Schrödinger equation in its hyper-geometric form

$$u(1-u)\,\omega"(u)+\left(1-\frac{ik}{\alpha}\right)(1-2u)\,\omega'(u)-\left(-\frac{ik}{\alpha}-s\right)\left(-\frac{ik}{\alpha}+s+1\right)\omega(u)=0. \tag{C.19}$$

The exact solution of the problem is the wave function

$$\Psi=\left(1-\xi^2\right)^{-\frac{ik}{2\alpha}}F\left[-\frac{ik}{\alpha}-s,-\frac{ik}{\alpha}+s+1,\,1-\frac{ik}{\alpha},\,\frac{1}{2}(1-\xi)\right] \tag{C.20}$$

finite for $\xi=1$ (i.e. for $x\to\infty$). This solution satisfies the condition that, as $x\to\infty$, $1-\xi\to 2e^{-2\alpha x}$. Indeed,

$$(1-\xi)=(1-\tanh(\alpha x))=\frac{\cosh(\alpha x)-\sinh(\alpha x)}{\cosh(\alpha x)}=\frac{2e^{-2\alpha x}}{e^{\alpha x}+e^{-\alpha x}}, \tag{C.21}$$

so for $x\to\infty$,

$$(1-\xi)=lim_{x\to\infty}\left(\frac{2e^{-2\alpha x}}{1+e^{-\alpha x}}\right)=2e^{-2\alpha x}. \tag{C.22}$$

Physically, this means that as x tends towards infinity, the wave function should only include the transmitted wave (which is proportional to $\exp(ikx)$). The asymptotic form of the wave function as $x\to\infty$ ($\xi\to 1$) (i.e., the wave function before the barrier) is found by transforming the hyper-geometric function [eq:exact solution] with the aid of formula *e7* in appendix *e* of Landau and Lifshitz' book [6].

$$\begin{aligned}\Psi=\left(1-\xi^2\right)^{-\frac{ik}{2\alpha}}\Bigg[&\frac{\Gamma\left(1-\frac{ik}{\alpha}\right)\Gamma\left(\frac{ik}{\alpha}\right)}{\Gamma(s+1)\,\Gamma(s)}F\left(-\frac{ik}{\alpha}-s,s+1-\frac{ik}{\alpha},1-\frac{ik}{\alpha},\frac{1}{2}(1-\xi)\right)+\\&+\left[\frac{1}{2}(1-\xi)\right]^{\frac{ik}{\alpha}}\frac{\Gamma\left(1-\frac{ik}{\alpha}\right)\Gamma\left(-\frac{ik}{\alpha}\right)}{\Gamma\left(-\frac{ik}{\alpha}-s\right)\Gamma\left(s+1-\frac{ik}{\alpha}\right)}F\left(s+1,-s,1+\frac{ik}{\alpha},\frac{1}{2}(1-\xi)\right)\Bigg]\end{aligned} \tag{C.23}$$

when $x\to-\infty$, $\xi\to-1$ qnd $F\to 1$. As $\left(1-\xi^2\right)^{-\frac{ik}{2\alpha}}=\left(1-\tanh(x\alpha)^2\right)^{-\frac{ik}{2\alpha}}=\cosh(\alpha x)^{\frac{ik}{\alpha}}=\left(\frac{e^{\alpha x}+e^{-\alpha x}}{2}\right)^{\frac{ik}{\alpha}}$, and

$$\left[\frac{1}{2}(1-\xi)\right]^{\frac{ik}{\alpha}} = \frac{(1-\xi)^{-\frac{ik}{2\alpha}}(1+\xi)^{\frac{ik}{2\alpha}}}{2^{\frac{ik}{\alpha}}} = \frac{1}{2^{\frac{ik}{\alpha}}}\left(\frac{1+\xi}{1-\xi}\right)^{\frac{ik}{2\alpha}} = \frac{(e^{\alpha x})^{\frac{ik}{2\alpha}}}{2^{\frac{ik}{\alpha}}}. \quad \text{(C.24)}$$

When $x \to -\infty$, $\left(1-\xi^2\right)^{-\frac{ik}{2\alpha}} \to \left(\frac{e^{-\alpha x}}{2}\right)^{\frac{ik}{\alpha}} = \frac{e^{-ikx}}{2^{\frac{ik}{\alpha}}}$, and $\left[\frac{1}{2}(1-\xi)\right]^{\frac{ik}{\alpha}} \to \frac{e^{ikx}}{2^{\frac{ik}{\alpha}}}$, which leads to

$$\Psi = \frac{1}{2^{\frac{ik}{\alpha}}}e^{-\frac{ik}{\alpha}}\frac{\Gamma\left(1-\frac{ik}{\alpha}\right)\Gamma\left(\frac{ik}{\alpha}\right)}{\Gamma(s+1)\Gamma(s)} + \frac{1}{2^{\frac{ik}{\alpha}}}e^{\frac{ik}{\alpha}}\frac{\Gamma\left(1-\frac{ik}{\alpha}\right)\Gamma\left(-\frac{ik}{\alpha}\right)}{\Gamma\left(-\frac{ik}{\alpha}-s\right)\Gamma\left(s+1-\frac{ik}{\alpha}\right)}. \quad \text{(C.25)}$$

The wave function is composed of the reflected and transmitted waves which are, respectively, the first and second term of Eq. (C.25).

Reflection and transmission coefficients

From Eq. (C.25) it is possible to calculate the reflection coefficient of the potential barrier: it is enough to take the squared modulus of the ration of coefficients in this function -

$$\begin{aligned} R &= \frac{|\Gamma\left(\frac{ik}{\alpha}\right)|^2|\Gamma\left(-\frac{ik}{\alpha}-s\right)|^2|\Gamma\left(s+1-\frac{ik}{\alpha}\right)|^2}{|\Gamma(s+1)|^2|\Gamma(s)|^2|\Gamma\left(-\frac{ik}{\alpha}\right)|^2} \\ &= \frac{\frac{\pi}{\frac{k}{\alpha}\sin(\frac{\pi k}{\alpha})}|\Gamma\left(-\frac{ik}{\alpha}-s\right)|^2|\Gamma\left(s+1-\frac{ik}{\alpha}\right)|^2}{\frac{-s\pi}{\sin(\pi s)}\frac{(-\pi)}{s\sin(\pi s)}\frac{\pi}{\frac{k}{\alpha}\sin(\frac{\pi k}{\alpha})}} \\ &= \frac{\sin^2(\pi s)}{\pi^2}|\Gamma\left(-\frac{ik}{\alpha}-s\right)|^2|\Gamma\left(s+1-\frac{ik}{\alpha}\right)|^2. \end{aligned} \quad \text{(C.26)}$$

Here can be recognised

$$R = \frac{\sin^2(\pi s)}{\pi^2}\Gamma\left(-\frac{ik}{\alpha}-s\right)\Gamma\left(\frac{ik}{\alpha}-s\right)\Gamma\left(s+1-\frac{ik}{\alpha}\right)\Gamma\left(s+1+\frac{ik}{\alpha}\right)$$

as $\Gamma(z)$ $\Gamma(z')$ $\Gamma(1-z')$ $\Gamma(1-z)$

$$R = \frac{-\sin^2(\pi s)}{\sin\pi\left(\frac{ik}{\alpha}+s\right)\sin\pi\left(\frac{ik}{\alpha}-s\right)}$$

$$R = \frac{-\sin^2(\pi s)}{\left(\sin(\pi s)\cos\left(\pi\frac{ik}{\alpha}\right)+\cos(\pi s)\sin\left(\pi\frac{ik}{\alpha}\right)\right)\left(-\sin(\pi s)\cos\left(\pi\frac{ik}{\alpha}\right)+\cos(\pi s)\sin\left(\pi\frac{ik}{\alpha}\right)\right)}$$

$$R = \frac{-\sin^2(\pi s)}{\cos^2(\pi s)\sin^2\left(\pi\frac{ik}{\alpha}\right)-\sin^2(\pi s)\cos^2\left(\pi\frac{ik}{\alpha}\right)}. \quad \text{(C.27)}$$

Finally, the transmission coefficient is $D = 1 - R$

$$\begin{aligned} D =& \frac{\cos^2(\pi s)\sin^2\left(\pi\frac{ik}{\alpha}\right) - \sin^2(\pi s)\cos^2\left(\pi\frac{ik}{\alpha}\right) + \sin^2(\pi s)}{\cos^2(\pi s)\sin^2\left(\pi\frac{ik}{\alpha}\right) - \sin^2(\pi s)\cos^2\left(\pi\frac{ik}{\alpha}\right)} \\ =& \frac{\cos^2(\pi s)\sin^2\left(\pi\frac{ik}{\alpha}\right) - \sin^2(\pi s)\left[\cos^2\left(\pi\frac{ik}{\alpha}\right) - 1\right]}{\cos^2(\pi s)\sinh^2\left(\pi\frac{k}{\alpha}\right) - \sin^2(\pi s)\cosh^2\left(\pi\frac{k}{\alpha}\right)} \\ =& \frac{\sin^2\left(\pi\frac{ik}{\alpha}\right)\left[\cos^2(\pi s) + \sin^2(\pi s)\right]}{\sinh^2\left(\pi\frac{k}{\alpha}\right) - \sin^2(\pi s)\sinh^2\left(\pi\frac{k}{\alpha}\right) + \sin^2(\pi s)\cosh^2\left(\pi\frac{k}{\alpha}\right)} \\ =& \frac{\sinh^2\left(\pi\frac{k}{\alpha}\right)}{\sinh^2\left(\pi\frac{k}{\alpha}\right) + \sin^2(\pi s)} = \frac{\sinh^2\left(\pi\frac{k}{\alpha}\right)}{\sinh^2\left(\pi\frac{k}{\alpha}\right) + \cos^2\left(\pi\left(s + \frac{1}{2}\right)\right)} \\ D =& \frac{\sinh^2\left(\pi\frac{k}{\alpha}\right)}{\sinh^2\left(\pi\frac{k}{\alpha}\right) + \cos^2\left(\frac{1}{2}\pi\sqrt{1 - \frac{8mU_0}{\hbar^2\alpha^2}}\right)} \end{aligned} \tag{C.28}$$

f $\frac{8mU_0}{\hbar^2\alpha^2} < 1$, or, in the opposite case,

$$D = \frac{\sinh^2\left(\pi\frac{k}{\alpha}\right)}{\sinh^2\left(\pi\frac{k}{\alpha}\right) + \cos^2\left(\frac{1}{2}\pi\sqrt{\frac{8mU_0}{\hbar^2\alpha^2} - 1}\right)}. \tag{C.29}$$

Useful gamma-functions properties

$$\begin{aligned} \Gamma(s+1) =& s\Gamma(s) \\ \Gamma(-s) =& \frac{\pi}{\sin(\pi s)\, s\Gamma(s)} \\ \Gamma(1-s)\Gamma(s) =& \frac{\pi}{\sin(\pi s)} \\ |\Gamma(s)|^2 =& \frac{-\pi}{s\sin(\pi s)} \\ |\Gamma(is)|^2 =& \frac{\pi}{s\sin(\pi s)} \\ \Gamma(s)^* =& \Gamma\left(s^*\right) \end{aligned} \tag{C.30}$$

if $s \in \mathbb{R}$.

References

1. J.O. Smith, *Mathematics of the Discrete Fourier Transform (DFT)* (W3K Publishing, 2007) http://www.w3k.org/books/
2. J.J. Hopfield, Theory of the contribution of excitons to the complex dielectric constant of crystals. Phys. Rev. **112**(5), 1555–1567 (1958)
3. S. Finazzi, I. Carusotto, Kinematic study of the effect of dispersion in quantum vacuum emission from strong laser pulses. Eur. Phys. J. Plus **127**(7) (2012)
4. S. Finazzi, I. Carusotto, Quantum vacuum emission in a nonlinear optical medium illuminated by a strong laser pulse. Phys. Rev. A **87**(2) (2013)
5. M. Jacquet, F. König, Quantum vacuum emission from a refractive-index front. Phys. Rev. A **92**(2) (2015)
6. L.D. Landau, E.M. Lifšic, Quantum mechanics: non-relativistic theory, in *Course of Theoretical Physics*, vol. 3, ed. by L.D. Landau, E.M. Lifshitz (Elsevier, Singapore, 3). ed., rev. and enl., authorized engl. reprint ed edition, 2007. OCLC: 837367864

Author Biography

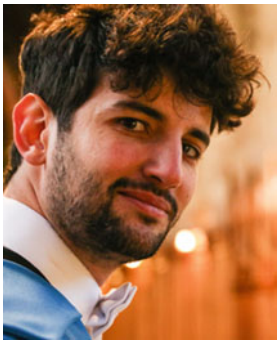

Maxime Jules Jacquet

Maxime (born 28 January 1990) is a natural philosopher whose primary research interest is the interplay between Quantum Physics and General Relativity.

In his youth, he enjoyed attending a wide range of public, free state schools until he graduated with a Scientific Baccalauréat in 2008. Still enjoying free tuition, he went on to study engineering at the Polytechnic School of the University of Orléans, France. He spent the academic year 2010–2011 in England via a newly inaugurated partnership between the Universities of Orléans and Staffordshire, UK. Upon returning to France to finish his engineering degree, he decided to specialise in Photonics. In 2013, he went back to the UK to undertake an MSc in Photonics at St Andrews and Heriot-Watt Universities.

That is where he met Friedrich König, with whom he studied toward his Ph.D. at St Andrews between 2013 and 2017. In those three and a half years, he used the tools of Quantum Field Theory on curved spacetime to study the kinematics of waves at optical event horizons in dispersive media. He also conducted experimental investigations of the scattering of classical waves on optical horizons created by few-cycle pulses in photonic crystal fibres. Once more, he was fortunate to be supported in

M. J. Jacquet, *Negative Frequency at the Horizon*, Springer Theses,
https://doi.org/10.1007/978-3-319-91071-0

his efforts by public funds, via an EPSRC grant and a 600th Anniversary Fellowship of the University of St Andrews.

From the very onset of his research career, Maxime has considered that the scientific endeavour is twofold: the advancement of knowledge must be shared with others, be it in discussions, teaching and/or outreach activities. He has always enjoyed actively taking part in the teaching activities of his host institution. He invariably found these experience to be enriching, and to be invaluable occasions to learn more about, and reflect on, his teaching as well as his learning philosophy and practices.

After his Ph.D., Maxime's academic peregrinations took him to the University of Vienna, where he opened his research horizons to new maps between theoretical physics and the physical world via foundational studies on time, entanglement, superposition and causal structures. For this young researcher, this is only the beginning of a journey in which experimental and theoretical studies promise to continuously collude.

Publications

2017 Analytical description of spontaneous emission
of light at the optical event horizon
with F. König—arXiv:1709.03100

2016 Supercontinuum generation in optical fibers
with G. Genty, M. Närhi and C. Amiot
https://doi.org/10.3254/978-1-61499-647-7-233
Proceedings of the International School of Physics Enrico Fermi

2015 Quantum vacuum emission at a refractive-index front
with F. König—https://doi.org/10.1103/PhysRevA.92.023851
Physical Review A **92**, 023851
Quantum vacuum emission from a moving refractive index front
with F. König—https://doi.org/10.1117/12.2187987
Proceedings of SPIE: Quantum Communications and Quantum Imaging

2013 Quantum Vacuum emission at the event horizon
MSc Thesis, Universities of St Andrews, Heriot-Watt and Orléans